Available online at www.sciencedirect.com
SCIENCE DIRECT®
Acta Biomaterialia xxx (2004) xxx–xxx
Acta BIOMATERIALIA
www.actamat-journals.com

Effects of polar solvents on the fracture resistance of dentin: role of water hydration

R.K. Nalla [a], M. Balooch [b], J.W. Ager III [a], J.J. Kruzic [a], J.H. Kinney [c], R.O. Ritchie [a,*]

[a] *Materials Sciences Division, Lawrence Berkeley National Laboratory, and Department of Materials Science and Engineering, University of California, 381 Hearst Memorial Mining Building, MC 1760, Berkeley, CA 94720, USA*
[b] *Department of Preventive and Restorative Dental Sciences, University of California, San Francisco, CA 94143, USA*
[c] *Lawrence Livermore National Laboratory, Livermore, CA 94550, USA*

Received 18 June 2004; received in revised form 24 August 2004; accepted 30 August 2004

Abstract

Although healthy dentin is invariably hydrated in vivo, from a perspective of examining the mechanisms of fracture in dentin, it is interesting to consider the role of water hydration. Furthermore, it is feasible that exposure to certain polar solvents, e.g., those found in clinical adhesives, can induce dehydration. In the present study, in vitro deformation and fracture experiments, the latter involving a resistance-curve (R-curve) approach (i.e., toughness evolution with crack extension), were conducted in order to assess changes in the constitutive and fracture behavior induced by three common solvents—acetone, ethanol and methanol. In addition, nanoindentation-based experiments were performed to evaluate the deformation behavior at the level of individual collagen fibers and ultraviolet Raman spectroscopy to evaluate changes in bonding. The results indicate a reversible effect of chemical dehydration, with increased fracture resistance, strength, and stiffness associated with lower hydrogen bonding ability of the solvent. These results are analyzed both in terms of intrinsic and extrinsic toughening phenomena to further understand the micromechanisms of fracture in dentin and the specific role of water hydration.

Keywords: Dentin; Fracture toughness; R-curve; Dehydration; Hydrogen bonding

1. Introduction

Dentin, the mineralized tissue that makes up the bulk of the tooth, is a hydrated bio-composite of type-I mineralized collagen fibers and nanocrystalline hydroxyapatite in its natural state. Human dentin is typically composed of ~45 vol.% of carbonated apatite mineral (~5 nm thick crystallites), and ~30 vol.% type-I collagen fibrils (typically 50–100 nm diameter), with an aqueous fluid making up the remaining 25%. On the ultrastructural level, the mineral is usually distributed in two sites, explicitly ~70–75% as extrafibrillar mineral (outside the fibrils) and the rest as intrafibriallar mineral (within the fibrils) [1], while the collagen molecule triple helices (roughly 280 nm long) form a staggered structure within the fibrils with a periodicity of approximately 67 nm. At a larger size scale, the most distinctive feature of the microstructure of dentin is the distribution of cylindrical tubules (1–2 μm diameter) that run from the dentin-enamel junction into the soft, interior pulp [2]. A majority (~75%) of the dentinal fluid is believed to lie within the tubules themselves, with the rest being distributed within the intertubular matrix [3].

Both intra- and interchain hydrogen bonding within the triple helices has long been thought to play an important role in forming the structure of collagen mol-

* Corresponding author. Tel.: +1 510 486 5798; fax: +1 510 486 4881.
E-mail address: roritchie@lbl.gov (R.O. Ritchie).

1742-7061/$ - see front matter © 2004 Published by Elsevier Ltd. on behalf of Acta Materialia Inc.
doi:10.1016/j.actbio.2004.08.002

ecules, along with a highly ordered inner hydration layer of water molecules which forms hydrogen bonds along the peptide chains [4–8]. Additionally, water has been shown to form hydrogen-bonded "bridges" which further contribute to the structure of collagen by forming intra- and interchain links within molecules, along with intermolecular bridges between neighboring triple helices [9,10] which presumably contribute to the structure and properties of the collagen fibrils.

The prime motivation for the current work is to develop a mechanistic understanding of the mechanical properties of dentin and, in particular, how these properties are influenced by microstructural modifications which may occur from caries, sclerosis, aging and restorative processes. Previously, it has been shown that the fracture resistance of dentin is lower in the absence of water (in vacuo) [11], suggesting that the role water plays in forming the molecular and fibrillar structure of collagen has an effect on the fracture properties. In order to further the understanding of how water affects the fracture resistance of dentin, the present study focuses on the fracture resistance of dentin where the water has been replaced by various polar solvents. Such behavior is of clinical interest as polar solvent-based adhesive monomers are often used in clinical dentistry to help achieve micromechanical retention of resin composites [12]. Although direct exposure of dentin to such solvents is quite rare, usage during the restoration process can cause inadvertent exposure, albeit for brief periods of time.

Previous investigations using demineralized dentin have shown that the removal of water through chemical dehydration, i.e., by replacing it with polar solvents such as methanol, acetone and ethanol, causes shrinkage of the tissue [13,14]. Furthermore, measurements of the elastic properties showed increased tensile moduli and ultimate tensile strength (UTS) levels when demineralized dentin was exposed to such solvents (as compared to behavior in water). Such stiffening and strengthening of dentin was attributed to increased levels of interpeptide hydrogen bonding between adjacent collagen fibrils [13–15] as the collagen structure was disrupted by the substitution of solvent for water molecules. These studies further revealed that the amount of shrinkage and the increase in modulus and tensile strength (UTS) were inversely proportional to the hydrogen bonding ability of the solvent, as measured by the Hansen solubility parameter (HSP) for hydrogen bonding, δ_H [16]. Water, on the other hand, with a relatively high δ_H value as compared to the polar solvents, "plasticized" collagen by breaking the interpeptide bonds, leading to a lower modulus and strength [13].

While effects of dehydration by anhydrous solvents on the tensile properties of demineralized dentin have been investigated, it is likely that these changes will also influence the fracture behavior of the natural, mineralized tissue; indeed, previous studies have indicated a critical role of water in determining the fracture resistance of dentin [11,17]. Consequently, the present study aims to investigate the fracture toughness behavior of dentin dehydrated chemically using three common polar solvents—acetone, methanol and ethanol, using a resistance-curve (R-curve) fracture mechanics approach. An R-curve approach is used to permit distinction between intrinsic toughening mechanisms, which affect crack initiation, and extrinsic mechanisms, which affect subsequent crack growth, the later mechanisms in dentin being largely associated with crack bridging [11,18]. In addition, the effects on the elastic properties at the macroscopic and the microscopic (fibrillar) levels are examined, and UV Raman spectroscopy is used to provide evidence that changes in collagen bonding are induced by the solvents.

2. Experimental procedures

2.1. Materials

Recently harvested fractured shards of elephant tusk taken from an adult male elephant (*Loxodonta africana*) were examined in this study; the bulk of this material is composed of dentin. The characteristic feature of elephant tusk dentin is the tubules that run through a matrix formed by the mineralized collagen fibers. Although extensive microstructural studies on elephant dentin have not been performed, its microstructure is similar to human dentin, although the dentinal tubules have a slightly larger diameter [19]. Our own observations indicated that the tubules are more elliptical in shape and the peritubular cuffs are much smaller or non-existent, although the tubule density (based on metallographic and synchrotron X-ray computed tomographic (SRCT) observations) and mineral content (based on SRCT observations) appear to be similar to human dentin.

To measure the toughness, nine ($N = 9$) compact-tension, C(T), specimens, were machined from the shards with specimen thicknesses of $B \sim 1.2$–3.1 mm, widths of $W \sim 13$–17.8 mm and initial notch lengths of $a_0 \sim 3.1$–5.4 mm. [1] The samples were oriented such that the nominal crack growth direction was perpendicular to the long axis of the tubules and the crack plane was in the plane of

[1] According to ASTM Standard E-399 [20], a state of plane strain is achieved when the sample thickness is greater than 2.5 $(K_c/\sigma_y)^2$ i.e., the thickness is significantly larger than the plastic or damage zone size of $\sim 1/2\pi\,(K_c/\sigma_y)^2$ where K_c is the fracture toughness and σ_y is the "yield" strength For elephant dentin, this would require samples thicknesses greater than approximately 1–3 mm to yield a plane-strain K_c value. However, as this criterion is generally quite conservative and the damage zone was well-contained within the specimen boundaries, it is believed that the toughness values measured with the current test specimens are very close to this lower-bound.

the tubules, as in our previous studies [11,18]. The specimens were polished to a 1200 grit finish, followed by polishing steps using a 1 μm alumina suspension and finally a 0.05 m alumina suspension. The notch was introduced with a slow-speed (~100 rpm) saw (TechCut II, Allied High Tech Products, Inc., Rancho Dominguez, CA). Finally, to permit easier initiation of a fatigue pre-crack, the machined notch was sharpened to a root radius of ~15 μm using a razor-micronotching technique (micronotch depth ~ 100 μm); the latter was achieved by repeatedly sliding a razor blade over the saw-cut notch using a custom-made rig, while irrigating with 1 μm diamond slurry. The specimens were then randomly divided into three groups. Each group was dehydrated prior to actual testing by soaking in a solvent (acetone, ethanol or methanol) for ~24 h at room temperature. The laboratory-grade solvents were obtained from two commercial vendors (methanol and ethanol/anhydrous alcohol from Mallinckrodt Baker Inc., Paris, KY; acetone from Burdick and Jackson, Muskegon, MI). The residual water content was 0.1%, 0.5% and 0.25% in methanol, ethanol and acetone, respectively, according to the manufacturers' specifications. The corresponding Hansen solubility parameters, δ_H, were obtained from Hansen's handbook [16].

2.2. Mechanical testing

2.2.1. Resistance-curve testing

R-curves on samples saturated with the various solvents were measured in ambient air (25 °C, 20–40% relative humidity) to evaluate the resistance to fracture in terms of the stress intensity, K, as a function of crack extension, Δa. The C(T) specimens were loaded in displacement control at a rate of ~0.015 mm/s using standard servo-hydraulic testing machines (MTS 810, MTS Systems Corp., Eden Prairie, MN) until the onset of cracking, which was determined by an initial drop in load. At this point, the sample was unloaded by 10–20% of the peak load to record the sample compliance at the new crack length. This process was repeated at regular intervals until the end of the test, at which point the compliance and loading data were analyzed to determine fracture resistance, K_R as a function of Δa. Crack lengths, a, were calculated from the load-line compliance data (measured using a linear variable-displacement transducer (LVDT) in the load frame) obtained during the test using standard C(T) load-line compliance calibrations [21]: [2]

$$a/W = 1.0002 - 4.0632U + 11.242U^2 - 106.04U^3 + 464.33U^4 - 650.68U^5, \quad (1)$$

where U is a fitting function written as

$$U = \frac{1}{(FC)^{1/2} + 1}. \quad (2)$$

C is the sample compliance and F is a calibration constant, taken to be that which gives the best agreement between the initial compliance and optically measured crack length at the beginning of the test. Due to crack bridging, errors can occur in the compliance-crack length measurements. Consequently, re-calibration to the actual crack length was performed periodically using optical microscopy (Olympus STM-UM measuring microscope, Olympus America Inc., Melville, NY; 0.5 μm resolution) to validate the measured crack lengths. Any discrepancies between the compliance and optically measured crack length were then corrected by assuming that the error accumulated linearly with crack extension over the growth interval; such a piecewise linear correction was performed over the extent of each test to account for the fact that most of the bridging developed in the early stages of the R-curve.

During the R-curve experiments, the samples were continuously irrigated with the corresponding solvent. The resulting $K_R(\Delta a)$ data were analyzed statistically using the non-parametric Kruskal–Wallis test, and were also subjected to regression analysis and Spearman non-parametric correlation against the Hansen parameter for hydrogen bonding, δ_H. The crack paths were examined after testing using optical microscopy and scanning electron microscopy (after coating with a gold–palladium alloy).

2.2.2. "Dehydrated/rehydrated/dehydrated" testing

Further "dehydrated/rehydrated/dehydrated" testing was performed on two specimens from each group (previously used for R-curve testing), wherein an R-curve test was initiated in one solvent (first "dehydrated" step), interrupted after some crack extension, and dried out in ambient air for ~24 h (to remove the solvent used). The samples were then rehydrated in Hanks' Balanced Salt Solution (HBSS) for ~24 h and tested while being continuously irrigated with HBSS ("rehydrated" step). After some crack extension, the samples were again dried out in ambient air for ~24 h (to remove water), dehydrated for ~24 h in the same solvent as earlier and tested while being continuously irrigated with that solvent (second "dehydrated" step). These experiments were conducted for the purpose of understanding the change in fracture resistance with chemical hydration/dehydration.

[2] The use of elastic compliance is a widely used technique in fracture mechanics testing to accurately measure crack length. The calibrations which relate compliance to crack length are valid for isotropic and anisotropic linear-elastic solids [21] and have been utilized successfully for numerous materials including dentin and bone [11,18].

2.2.3. Deformation behavior testing

To assess whether any changes in the fracture properties are reflective of changes in the deformation behavior (elastic and yielding properties), three-point bending strength tests were conducted. Specifically, unnotched, nominally flaw-free, beams of elephant dentin roughly 1.55–1.75 × 2.8–3.0 × 20 mm were sectioned (orientation same as for R-curve testing) from the fractured shards and polished as described previously. These beams were then soaked in one of the three solvents and in HBSS ($N = 3$ each) for ~24 h at room temperature prior to actual testing. The mechanical testing involved loading the beams to failure at a rate of ~0.015 mm/s under three-point bending (center-to-end loading span = 7.62 mm) using a standard servo-hydraulic testing machine (MTS 810, MTS Systems Corp., Eden Prairie, MN), while the loads (from the force transducer) and the load-line displacements (from the LVDT) were continuously monitored. The load-displacement data thus obtained were analyzed to assess differences in the deformation behavior in terms of the initial stiffness (reflective of Young's modulus) and ultimate (bending) strength.

2.3. Nanomechanical testing

To evaluate the elastic properties at the fibrillar level, "hydrated/dehydrated/rehydrated" experiments were performed. Small polished blocks of elephant dentin (~3 × 3 × 3 mm) were used for this purpose. These dentin samples were partially decalcified in 10% citric acid for 15 s, carefully rinsed with HBSS and then stored (short-term) in HBSS until actual testing. This procedure removes extrafibrillar mineral to a depth of ~750 nm [22] and thus, provides a surface layer, roughly 1 μm thick, of collagen fibril network (with the interfibrillar mineral almost intact), on the top of a smooth mineralized dentin substrate.

Nanoindentation tests were performed using an atomic force microscope, AFM (Nanoscope III, Veeco, Santa Barbara, CA), to which a force–displacement transducer (Triboscope Micromechanical Test Instrument, Hysitron Inc., Minneapolis, MN) was attached. A tungsten rod, 5 mm in length, with a diamond indenter (radius of curvature = 100 μm to sample several fibers and get an average value for the network) attached to it, was fitted to the transducer. The whole sample, diamond tip, and a portion of the tungsten rod were immersed in solvent during the tests. For elastic modulus determination (AFM in static mode), the loading curve involved engaging the indenter with the surface of the specimen, loading to a specific maximum load (40–100 μN) in 1.5 s, holding at the maximum load for 1.5 s, and then unloading at the same rate as the loading. Lower loads were used to limit the displacement under 500 nm to avoid non-linearity in the transducer response. The unloading load–displacement data thus obtained were used to determine the elastic modulus based on classical indentation theory introduced by Boussing (reviewed in Ref. [23]), simplified by Sneddon [24], and generalized by Pharr et al. [25]. According to this theory, a material experiences elastic recovery during the first 25% of unloading phase of the unloading portion of the load–displacement curve. The slope of the unloading curve close to maximum load provides a measure of the stiffness of the material, from which the reduced [3] elastic modulus can be determined if the tip geometry is defined [26]. Such measurements were made initially in HBSS, followed by a dehydrating solvent (acetone and ethanol were used), and finally after rehydrating with HBSS; nanoindentation was performed on three different samples for each group (water, acetone and ethanol), with ten individual load–displacement measurements being made on each sample. The modulus data for the collagen fiber network thus obtained were averaged to obtain mean values of the moduli.

2.4. UV Raman spectroscopy

Finally, to qualitatively evaluate whether the bonding within the collagen changes upon dehydration, Raman spectroscopy was performed. To avoid fluorescence interference and to resonantly enhance the organic signal with respect to that from the inorganic matrix, excitation in the deep ultraviolet was used. A continuous wave (cw) intracavity doubled, argon ion laser operating at 244 nm was used as the excitation source. The laser power at the sample was kept below 5 mW, and a custom-made rotating (~45 rpm) stage was used to avoid laser damage to the organic component. The laser was focused on the sample with an f/4 100 mm fused silica lens. Back-scattered light was collected with the same lens, collimated, and directed to the entrance slit of a UV-optimized triple spectrometer. Spectra were collected with a back-thinned CCD camera. Two specimens from each group (acetone, ethanol, methanol and HBSS) were randomly chosen for these experiments. Ten frames of 10 s exposure each were collected from each sample; comparison of the first and last frames from each set confirmed the sample stability under laser illumination. The spectral post processing procedure used was as follows: (1) averaging of the 10 frames and cosmic ray removal; (2) subtraction of a linear background obtained from the signal at 500 and 2000 cm^{-1},

[3] The reduced elastic modulus, E^* is given by $E^* = \left[\frac{(1-\nu_s^2)}{E_s} + \frac{(1-\nu_i^2)}{E_i}\right]^{-1}$, where E_s and E_i and ν_s and ν_i are the elastic moduli and Poisson's ratios of the specimen and the indenter, respectively. Since the elastic modulus of the specimen is significantly lower than that of the diamond indenter ($E_i \to \infty$), this reduces to $E^* \approx \left[\frac{(1-\nu_s^2)}{E_s}\right]^{-1}$.

where little Raman scattering from the sample is expected; (3) nine-point running averaging smoothing and normalization to the height of the CH_2 wag peak at 1450 cm^{-1}. The position and normalized height of the amide peaks (which are reflective of conformation of the organic matrix [27]) vs. the solvent δ_H were then evaluated using simple regression analysis.

3. Results

3.1. Resistance-curve behavior

Load–displacement data obtained during the R-curve tests were analyzed to evaluate the resistance to fracture in terms of the stress intensity, K, as a function of crack extension, Δa; the resulting R-curves for the chemically dehydrated dentin for all three test groups (acetone, ethanol, methanol) are shown in Fig. 1. Also included are data ($N = 5$) for hydrated elephant dentin (tested in HBSS) from a previous study [11]. Cracks can be seen to grow subcritically for crack extensions of ~4–5 mm (except for one of the specimens of the acetone group) prior to the conclusion of the tests. All the R-curves showed a linearly rising behavior initially, followed by a flat "plateau", similar in appearance to that previously reported for similar tests in HBSS [11]. The extent of crack growth (~4–5 mm) was chosen such that the majority of samples had reached the "plateau" toughness, after which the fracture resistance was observed to be essentially constant.

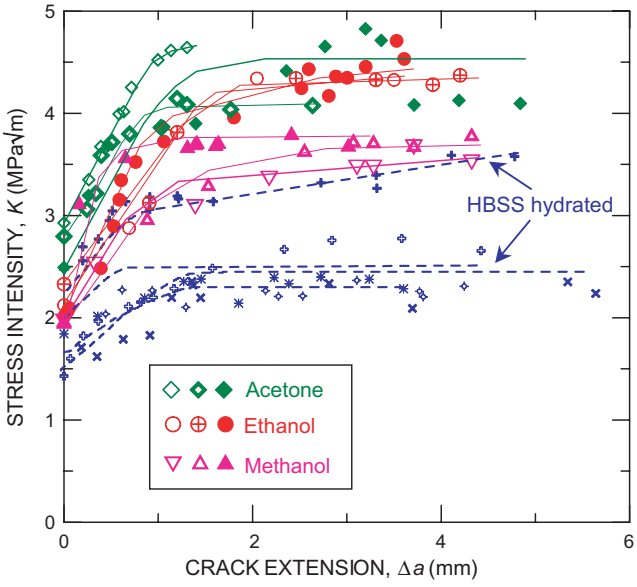

Fig. 1. Fracture resistance of dentin for chemically dehydrated dentin tested in acetone, ethanol and methanol expressed in terms of resistance curves. Data for hydrated dentin (dotted lines) are shown from a previous study [11].

The general trend shown by these data is that the fracture toughness is progressively increased in dentin chemical dehydrated with the solvents methanol, ethanol and acetone, all compared to HBSS hydrated dentin. This trend is seen with both crack-initiation and crack-growth toughness. Specifically, values of the crack-initiation toughness, K_0 obtained by extrapolating a linear fit to the initial rising part of the R-curve to the point of zero crack extension ($\Delta a = 0$), were, respectively, (mean ± SD) 1.95 ± 0.01, 2.16 ± 0.16 and 2.74 ± 0.22 MPa $\sqrt{m}$ for methanol, ethanol and acetone. All of these values are higher than the 1.88 ± 0.40 MPa $\sqrt{m}$ reported for the HBSS hydrated specimens in our previous study using dentin from the same elephant [11]. The Kruskal–Wallis statistical test revealed that differences in the K_0 data were significant ($p = 0.04$). With respect to crack-growth toughness, the initial slope of the R-curves can be seen to be monotonically rising in all the cases, with slopes of, respectively, 0.98 ± 0.24, 1.32 ± 0.27 and 1.43 ± 0.42 MPa $\sqrt{m/mm}$, observed for methanol, ethanol and acetone, as compared to 0.54 ± 0.16 MPa $\sqrt{m/mm}$ for hydrated (HBSS) dentin. The differences in these data were also significant ($p = 0.02$). Finally, all the R-curves were found to "plateau", respectively, at 3.66 ± 0.17, 4.39 ± 0.06 and 4.41 ± 0.32 MPa $\sqrt{m}$ for methanol, ethanol and acetone, as compared to 2.58 ± 0.45 MPa $\sqrt{m}$ for hydrated (HBSS) dentin. These data were also significant ($p = 0.01$). Post hoc multiple comparison tests were not performed owing to the relatively small sample sizes involved. Similar increases were observed in a previous study of single-value fracture toughness values of bovine bone by Lucksanambool et al. [28].

Fig. 2 shows the initiation, growth and "plateau" toughnesses as a function of the Hansen solubility parameter for hydrogen bonding forces, δ_H. These plots reveal a clear trend of decreasing fracture toughness with increasing ability of the solvent to form hydrogen bonds. The coefficient of determination, R^2, values for the exponential regressions shown in the plots were quite high for the growth and plateau toughnesses ($R^2 = 0.49$, 0.73, and 0.80 for initiation, growth and plateau toughness, respectively). Spearman correlation coefficients, r, were also relatively high ($r = -0.77$, -0.85 and -0.92 and the relationships were significant ($p = 0.001$, <0.0001 and <0.0001) for the initiation, growth and plateau toughness, respectively.

3.2. "Dehydrated/rehydrated/dehydrated" testing

In corresponding "dehydrated/rehydrated/dehydrated" tests shown in Fig. 3, where the degree of chemical hydration for each of the three solvents was changed during the course of the test, rehydration with HBSS was observed to markedly lower the maximum load sus-

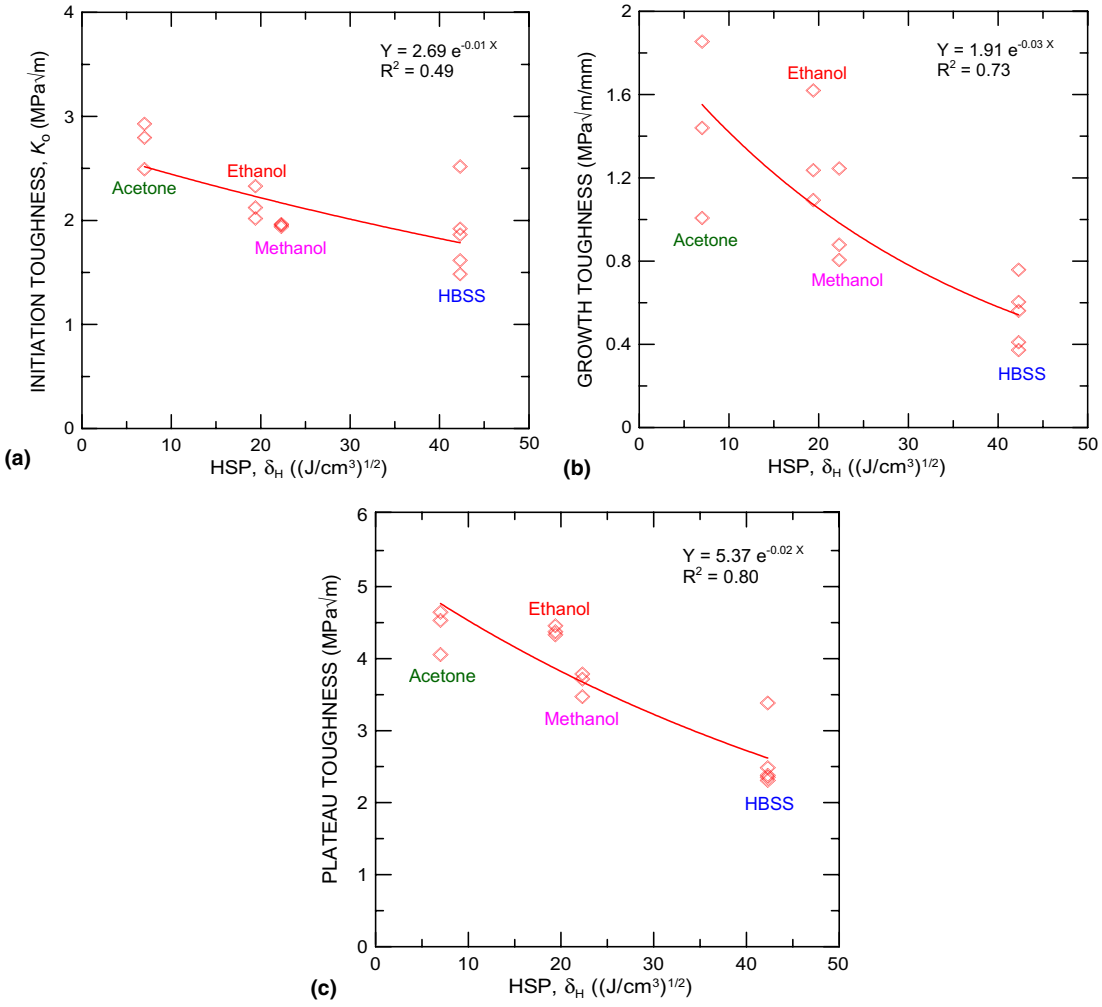

Fig. 2. Variation of (a) initiation, (b) growth, and (c) plateau toughness with Hansen Solubility Parameter (HSP) for hydrogen bonding forces, δ_H. The HSP for water was used for HBSS. The exponential fit for the data and the corresponding coefficient of determination, R^2, are given at the top right corner of each plot.

tained by the specimen, with corresponding lowering of the R-curve toughness. On subsequent dehydration, the toughness was observed to increase back to the original levels and the specimens were observed to behave very much like in the first dehydrated segment of the test. The magnitude of this effect was largest in acetone and smallest in methanol.

3.3. Deformation and strength behavior

Typical load–displacement data for the three-point bending tests are shown in Fig. 4 for dentin tested in acetone, ethanol, methanol and HBSS for specimens of identical 1.65×2.9 mm cross-sectional dimensions (which allowed for direct comparison). Additional data for samples with slightly varied cross-sectional dimensions (±0.1 mm) showed the same trends, but are not compared in Fig. 4 as sample dimensions effect the load and displacement values. From this data, two distinctive trends are evident—the specimen stiffness (see Fig. 4), directly indicative of the global elastic modulus, increases upon chemical dehydration, as does the tensile strength (again, see Fig. 4). Indeed, the tensile strength when the specimens were dehydrated with acetone is almost double of that measured when hydrated. Furthermore, the amount of ductility/deformation that the dentin endured prior to fracture was reduced substantially upon dehydration with acetone and ethanol. Dehydration with methanol did not have any effect on the ductility, though the stiffness and the ultimate strength did increase substantially. [4]

[4] Note that the tests described in Fig. 4 are bend tests, and thus these comparisons are made on the basis of applied loads and displacements. For a fully quantitative assessment of the tensile strength and stiffness of dentin in these solvents, the reader is referred to Ref. [15].

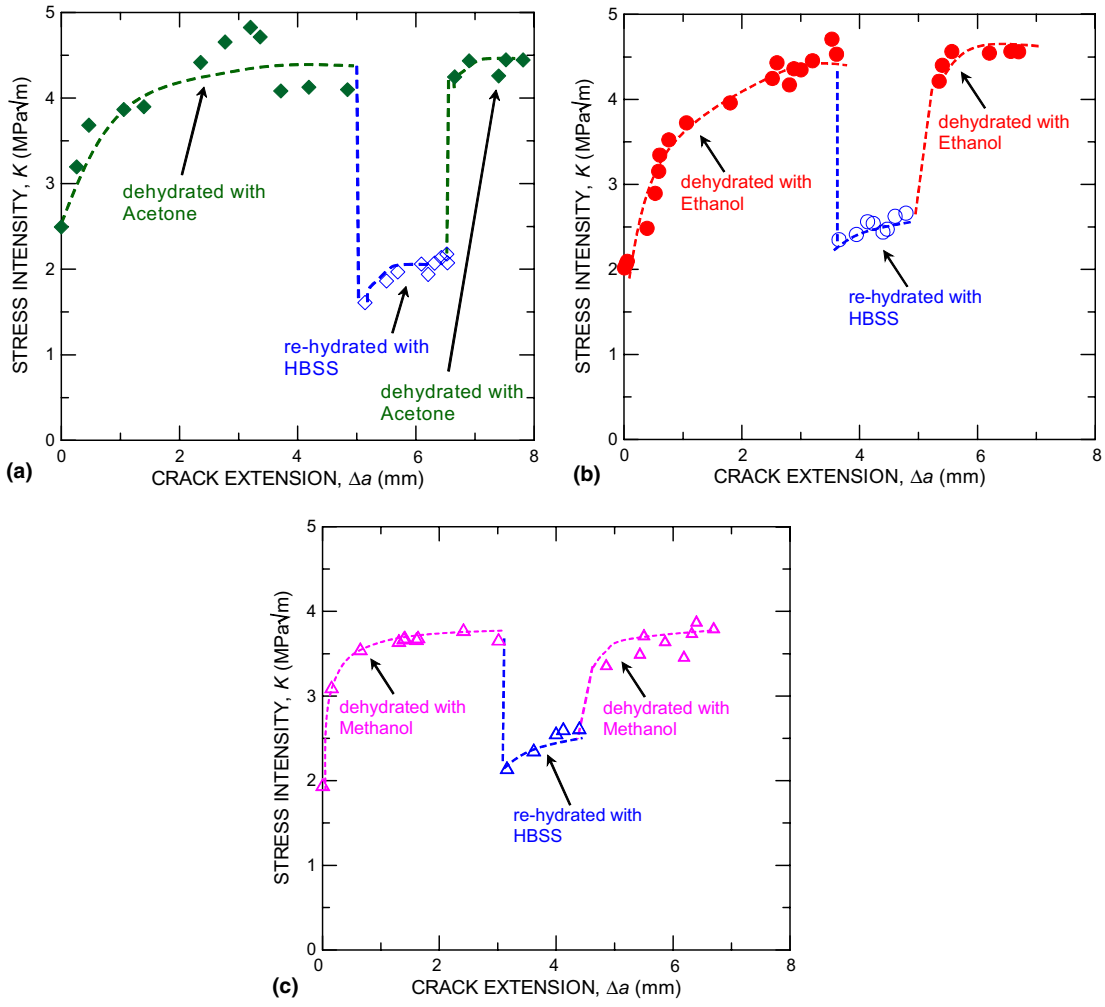

Fig. 3. Results of the "dehydrated/rehydrated/dehydrated" tests for (a) acetone, (b) ethanol, and (c) methanol expressed in terms of R-curve behavior. Note the reduction in toughness in all three cases when exposed to water (HBSS).

3.4. Nanomechanical behavior

Fig. 5a shows a typical micrograph of the ultrastructure of hydrated dentin obtained by atomic force microscopic imaging; attempts to image under other solvents were not successful. The network that the collagen fibers form can be seen from the low resolution AFM image (left panel in Fig. 5a); the higher resolution image (right panel in Fig. 5a) revealed the 67 nm periodicity, characteristic of type-I collagen [1]. These images suggest that the demineralization treatment removed predominantly only the extrafibrillar mineral, leaving structurally-intact collagen fibers that can be used for AFM-based nanoindentation. Fig. 5b shows typical "hydrated/dehydrated/rehydrated" nanoindentation data obtained for the collagen fiber network; the dehydration in this case was performed in acetone. The elastic moduli deduced from such load–displacement curves were ~40 MPa in water, increasing to ~1500 MPa in acetone, and reduced back to ~30 MPa upon rehydration in water. Additionally, representative data for the dehydration portion of the test for ethanol are also included in Fig. 5c; dehydration with ethanol resulted in similar, fully reversible increases in the reduced elastic moduli of individual collagen fibers, with values of ~1000 MPa obtained (Fig. 5c). Averaging such measured moduli gave mean (±SD) values of 100 ± 70 MPa in hydrated (HBSS) dentin, 1500 ± 500 MPa in acetone, 1100 ± 300 MPa in ethanol, and 70 ± 50 MPa in the rehydrated (HBSS) state. In addition, the shape of load–displacement curves suggest that the collagen network is highly viscoelastic in water, less so in ethanol and much less so in acetone. Indeed, a measurable load relaxation is observed during the 1.5 s peak hold during the indentation, which along with considerable hysteresis of the loading/unloading curve elucidates the viscoelastic behavior of the HBSS-hydrated dentin. For the ethanol case, some load relaxation and hysteresis is also seen during the indentation. Finally, for the acetone case, there is essentially no relaxation at the peak of the indentation, and the hysteresis is more

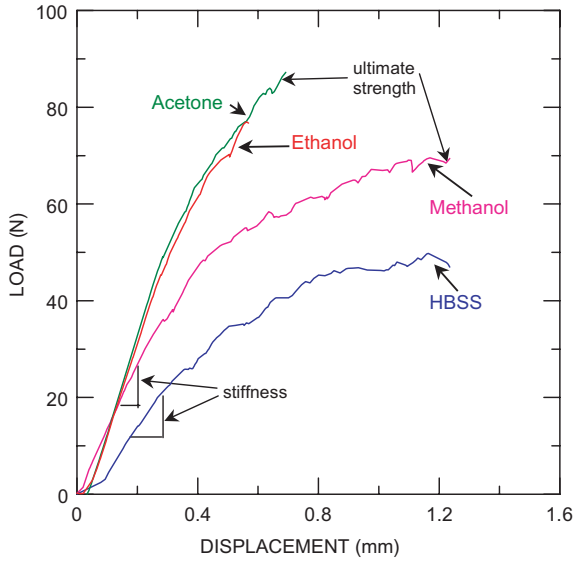

Fig. 4. Typical load–displacement data for chemically dehydrated (acetone, ethanol and methanol) and hydrated (HBSS) dentin. Note the increased strength levels in all the dehydrated cases. All tests ended with the specimen being fractured.

limited. Further investigation of these phenomena is currently being undertaken to develop an understanding of viscoelasticity at the fibrillar level in collagen. [5]

3.5. UV Raman spectroscopy

Fig. 6 shows typical Raman spectra for specimens from the four groups, i.e., dentin hydrated with HBSS and chemically-dehydrated with methanol, ethanol and acetone. The resonance enhancement of the peaks from the organic matrix is apparent in comparison to spectra reported using visible excitation (e.g., [29,30]). In particular, the PO_4^{3-} ν_1 peak at 960 cm^{-1}, which is dominant in visible Raman and FT-Raman spectra, is of relatively low intensity with 244 nm excitation. UV excitation leads to very distinct Raman peaks from the organic matrix. Based on reported visible Raman assignments for bone (e.g., see Ref. [29]), a compositionally similar mineralized tissue, three peaks can be definitively assigned here—amide III (~1247–1258 cm^{-1}), CH_2 wag (~1448–1459 cm^{-1}) and amide I (~1625–1643 cm^{-1}). The amide peaks, particularly amide I and amide III, are believed to be good indicators of protein conformation because of the role of the amide moiety in cross-linking and bonding [27]. Examination of the present data showed that both the height (as normalized to the height of the relatively invariant CH_2 wag peak) and location of the amide peaks varied with solvent group (Fig. 7). The height of both amide peaks decreased with increasing δ_H (Fig. 7a and b). The corresponding R^2 values for the exponential regressions, shown in the plots, were quite high ($R^2 = 0.81$ and 0.34 for amide I and amide III, respectively). The peak positions moved to higher frequency with increasing solvent δ_H (Fig. 7c and d), although the corresponding coefficients of determination, R^2, for the exponential regressions shown in the plots were comparatively low ($R^2 = 0.12$ and 0.17 for amide I and amide III, respectively) compared to those for the peak height. The excessive scatter (and the corresponding lower R^2 values) for the frequency shift does make assessment of the data difficult; [6] however, there is a definitive shift in the peak position to higher wave numbers when the data for the chemically dehydrated dentin are compared *as a whole* to that of hydrated dentin. These results suggest that the protein conformation in the organic matrix (which is ~90–95% collagen) does change as a function of the hydrogen bonding ability of the solvents.

4. Discussion

The R-curve fracture toughness results reported in this study (Figs. 1–3) clearly demonstrate that the fracture properties of elephant dentin are affected by the dehydration induced by three common polar solvents – methanol, ethanol and acetone. Furthermore, both the intrinsic toughness, which corresponds to the initiation toughness on the R-curve (Fig. 2a), as well as the extrinsic toughness, which is related to crack bridging [11,18] and is best measured by the crack-growth toughness (Fig. 2b), are related inversely to the hydrogen bonding ability of these solvents, as measured by the Hansen solubility parameter for hydrogen bonding, δ_H. Hansen solubility parameters have previously been used to rank penetrating/bonding capabilities of many common monomers and solvents used in adhesive dentistry (e.g., [31–35]). In addition to the contribution from hydrogen bonding, Hansen's semi-empirical approach included contributions from dispersive (δ_D) and polar forces (δ_P) [16]. Regression analyses for the toughness data vs. δ_D and δ_P, the Hansen solubility parameters for dispersive and polar forces, respectively, gave much lower correlation coefficients (data not included here).

[5] The viscoelastic properties of dentin, evaluated under step-function loading by observing the strain relaxation, suggest that the relaxation times are substantially lower than 1 s. In the present study, the loading/unloading time periods were significantly longer, implying that the (quasi-static) displacement rates used typically (between 30 and 270 nm/s) were so low that any viscoelastic contribution would be negligible.

[6] It should be noted that each data point in Fig. 7 is an average of 10 individual frames of 10 s each. Given that the samples were on a rotating stage, and the laser spot size was relatively large (~500 μm), sufficient sample sampling is believed to occur during the spectroscopic measurements.

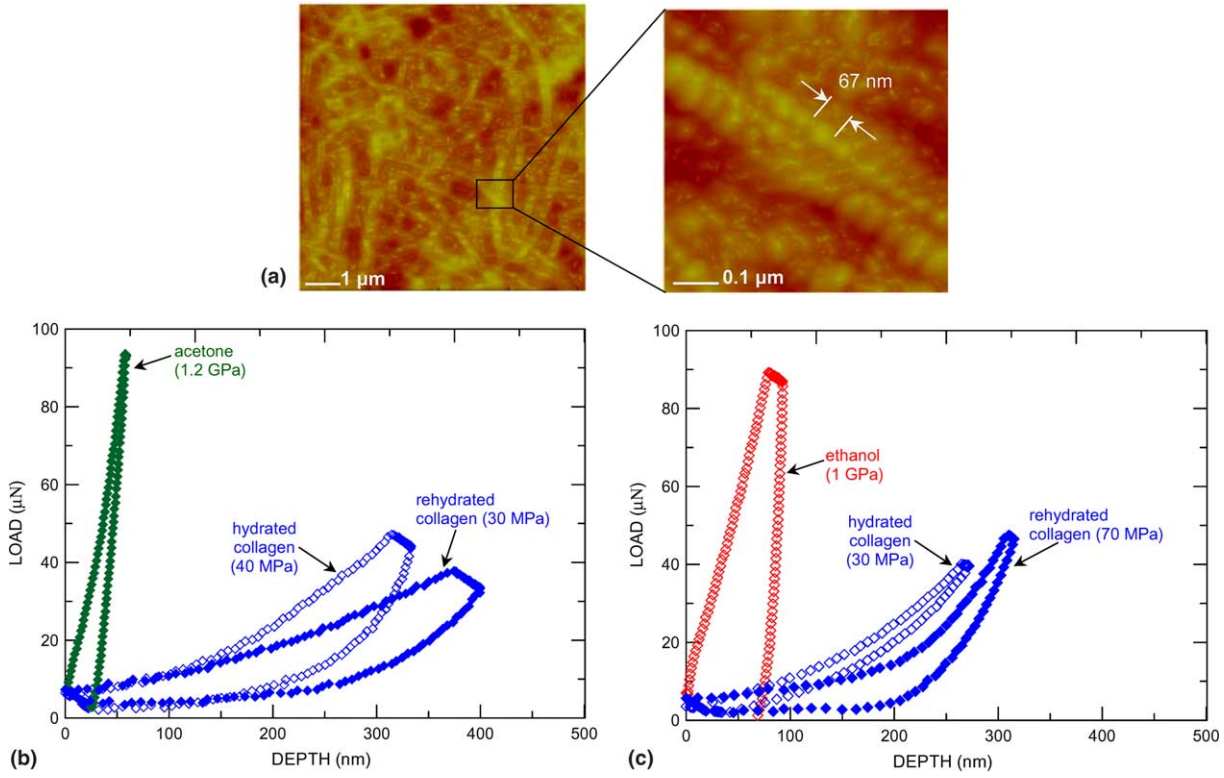

Fig. 5. (a) AFM images of hydrated collagen fibers. Note the regular "banded" structure as indicated in the higher magnification micrograph (left). Typical load–displacement data obtained for AFM-based "hydrated/dehydrated/rehydrated" nanoindentation of individual collagen fibers for the (b) water/acetone/water, and (c) water/ethanol/water cases are shown (numbers in brackets are calculated reduced elastic moduli). Note the dramatic increase in the modulus (slope of initial portion of the unloading curve) upon chemical dehydration.

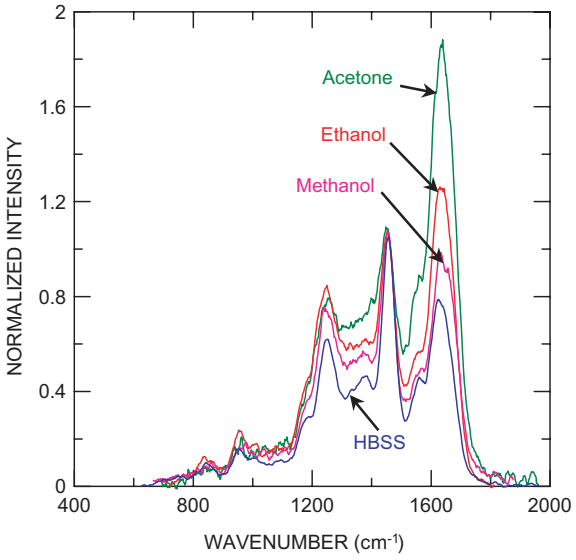

Fig. 6. Typical UV Raman spectra obtained for chemically dehydrated (acetone, ethanol and methanol) and hydrated (HBSS) dentin. Note the strong effect of dehydration on the relative intensity of the Amide I band (~1640 cm^{-1}).

The observed increase fracture resistance upon exposure to these polar solvents, however, was completely reversible upon rehydration, and furthermore, could be recovered again upon subsequent chemical dehydration. Increases in the stiffness and the ultimate strength levels at the macroscopic level were also observed from three-point bending tests (Fig. 4) similar to results previously reported for demineralized dentin [13,15]. Additionally, pico-force AFM nanoindentation measurements indicated that this increase in stiffness at the macroscopic level for solvents with low δ_H values percolates to the ultrastructural level where individual collagen fibrils demonstrated increased stiffness upon chemical dehydration; again, similar to the fracture resistance behavior, this effect was also reversible with subsequent rehydration.

These results, both at the ultrastructural and macroscopic levels, are in accord with trends observed for macroscopic tensile tests of fully demineralized dentin [13,15]. Pashley et al. [15] report average elastic moduli of, respectively, 11, 43 and 132 GPa in water, methanol and acetone, i.e. a 12-fold increase from water to acetone. The present measurements indicate a weaker effect with chemical dehydration of mineralized dentin; qualitative examination of Fig. 4 suggests that the modulus/stiffness changes by a factor of ~3 from HBSS to acetone. This may be expected since the modulus of composite materials are typically governed by a rule of

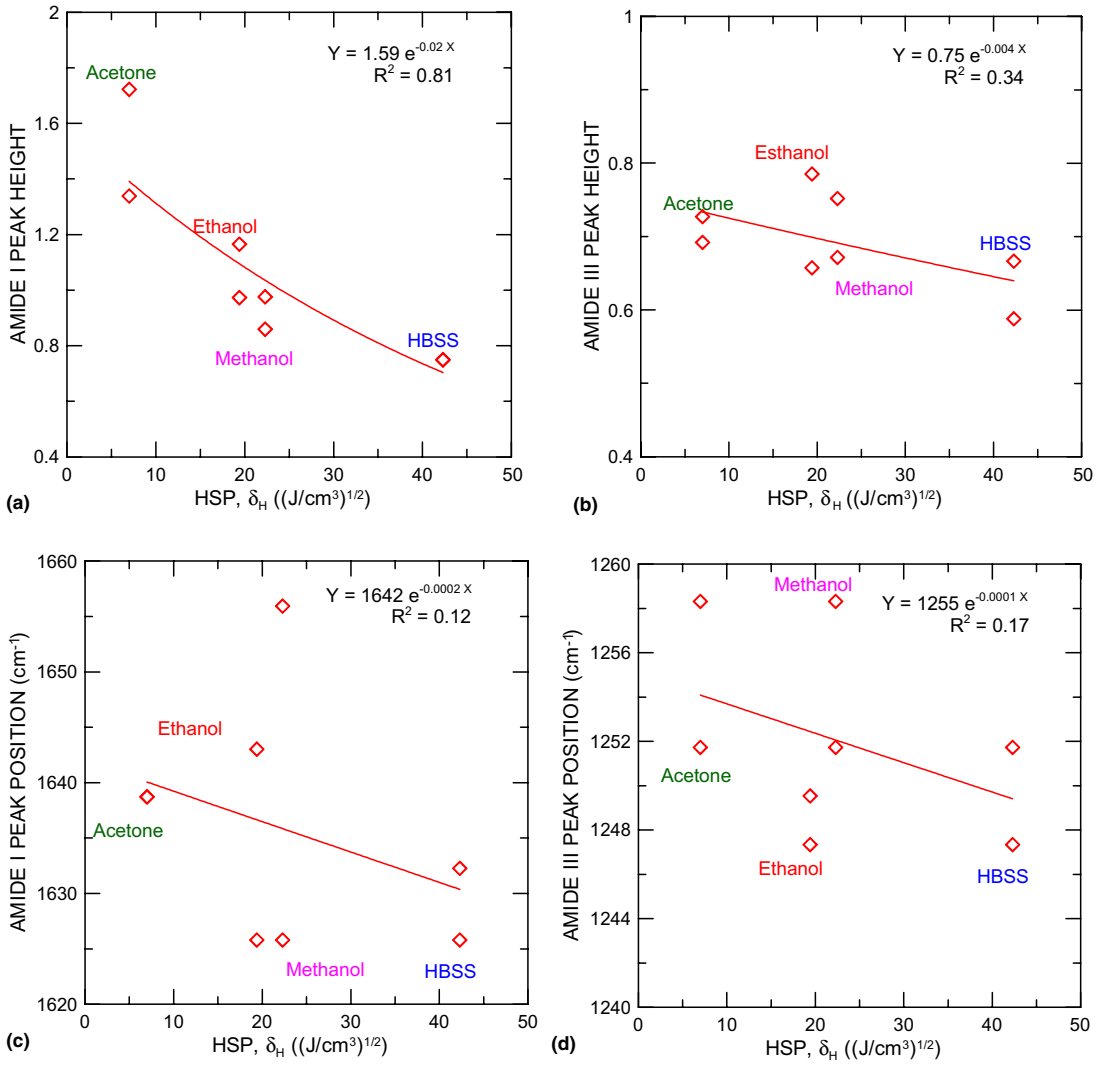

Fig. 7. Variation of the amide I and amide III peak positions and peak heights (normalized to the height of the CH_2 wag peak) with Hansen Solubility Parameter (HSP) for hydrogen bonding forces, δ_H. The exponential fit for the data and the corresponding coefficient of determination, R^2, are given at the top right corner of each plot.

mixtures, which is a volume weighted average of the component properties. Thus, the mineral in the present case should act to partially "shield" the collagen, i.e., taking on more of the load, making the total change in stiffness of the mineralized dentin less pronounced. The ultimate tensile strength showed an increase by a factor of ~2 both for mineralized (Fig. 4) and demineralized dentin [15] when comparing water-based solutions to acetone, and hence, the effect of dehydration on the strength does not appear to be affected as strongly by demineralization. Again, this is not surprising because the strengths of composite materials are typically not so dictated by the rule of mixtures (e.g., [36]).

Pashley et al. [15] have suggested that the increased stiffness and strength of demineralized dentin exposed to such solvents is the result of the formation of additional hydrogen bonds between adjacent collagen peptide chains. In the demineralized dentin, additional bonding is thought to cause the observed contraction of the tissue, while providing additional strength and stiffness [13–15]. This theory is consistent with the concept that the structure of collagen is governed in part by several factors relating to hydrogen bonding and water, such as direct intra- and interchain hydrogen bonding, an ordered hydration layer of water molecules occupying hydrogen bonding sites along the collagen molecules, and hydrogen bonded water "bridges" which form both intra- and interchain links, as well as spans between the collagen molecules [4–10]. Accordingly, the effect of replacing water with polar solvents with lower δ_H values would be expected to be twofold: (1) the collagen structure would be disrupted, and (2) less hydrogen bonding sites would be occupied by the weaker bond forming solvent. These additional, available

hydrogen bonding sites, coupled with the disrupted collagen structure, may then allow more direct hydrogen bonding between molecules. Furthermore, owing to the ease of breaking and re-formation of such bonds, it would be expected that changes in the properties should be reversible, consistent with observations in Figs. 3 and 5b. The resulting matrix would then be stiffer at the ultrastructural level (Fig. 5), and consequently, also at the macroscopic level (Fig. 4) as has been demonstrated in the present work for intact, mineralized dentin. An increase in direct collagen–collagen bonding also explains the shrinkage of the collagen matrix reported previously by Maciel et al. [13]. Finally, as mentioned in Section 3.5, changes in the vibrational spectrum were observed (Figs. 6 and 7), that were indicative of changes in the protein conformation. Such changes in the Raman spectrum could be the result of stronger collagen–collagen hydrogen bonding, as has been suggested by Gupta et al. [37] who observed similar frequency shifts for a number of pentapeptides. Further investigation into the exact nature of these changes is definitely warranted and is currently being undertaken.

It is possible that other mechanisms in addition to collagen–collagen bonding are contributing to the change in elastic properties in mineralized collagen. In particular, a "granular medium" model can be invoked to explain the observed increase in moduli with dehydration. Specifically, the architecture of normal hydrated dentin is considered to consist of stiff, mineralized collagen fibrils forming an open-celled network, which is surrounded by a protective granular matrix of nanocrystalline apatite particles (extrafibrillar mineral). The mineralized collagen fibrils are the largest contributors to the elastic properties. Upon dehydration, the fibrils contract slightly due to increased collagen–collagen hydrogen bonding (consistent with the matrix shrinkage reported by Maciel et al. [13]), placing the granular matrix into compression. This residual compressive stress consolidates the mineral grains and forces them into contact. We theorize that this contact, perhaps combined with the decreasing contact compliance from the elimination of the water, is responsible for the measurable increase in the Young's modulus with drying; this is currently being investigated.

The correlation of increased fracture resistance with decreasing Hansen solubility parameter for hydrogen bonding, akin to that seen for strength and stiffness, suggests that similar factors are contributing to the increased fracture properties. Indeed, one may expect that the intrinsic resistance to crack propagation in the HBSS hydrated case is limited by the ability of the collagen molecules to hold the tissue together, as is evidenced by the "pull-out" of collagen fibers in the crack wake [38]. When the water is replaced by polar solvents with lower δ_H values, the increased intermolecular hydrogen bonding between the collagen may

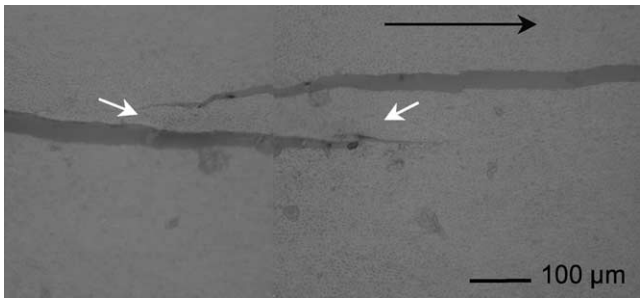

Fig. 8. Optical micrograph showing crack bridging by uncracked ligaments (indicated by white arrows) in dentin dehydrated using methanol. The black arrow indicates the nominal direction of crack growth.

then act to provide improved resistance to cracking. As for the extrinsic, or crack-growth, toughness, this behavior has been shown to be the result of intact bridges of material which span the crack wake (Fig. 8), limiting crack opening and sustaining some of the applied load which would otherwise go towards crack propagation [11,18]. By replacing water with polar solvents, these bridges would become stiffer and stronger, and accordingly further limit crack opening and sustain higher load levels. Although the tissue behavior appears to become more brittle in the low δ_H solvents, tendencies for premature bridge breakage due to increased brittleness would be offset, at least in part, by the higher strengths of the bridges. Furthermore, because the stiffness change is reversible, upon rehydration with HBSS, the extrinsic contribution to the fracture resistance returns to "normal" levels for the still intact bridges (Fig. 3). Thus, it appears that hydration affects both the intrinsic and extrinsic toughening behavior in dentin.

It is interesting to note that comparing the R-curve results obtained here with those reported previously for dentin dehydrated in vacuo [11], some qualitative and quantitative differences in the fracture behavior are observed (Fig. 9). Dentin dehydrated in vacuo showed a lower crack-initiation toughness, $K_0 = 1.18$ (SD = 0.20) MPa $\sqrt{m}$, as compared to 1.88 (SD = 0.40) MPa $\sqrt{m}$ for the hydrated (HBSS) specimens; furthermore, the slope of the R-curves for in vacuo dehydrated dentin was seen to be monotonically rising over 4–6 mm of crack extension and distinctly shallower (0.26 ± 0.05 MPa $\sqrt{m}$/mm) than for hydrated dentin, which displayed an initially steep slope (0.54 ± 0.16 MPa $\sqrt{m}$/mm) followed by a "plateau" region. This difference in behavior was previously rationalized based on the observation of extensive crack blunting, owing to plastic and viscoplastic (creep) deformation processes in the vicinity of the crack tip in hydrated dentin, and was in contrast to dentin dehydrated in vacuo where the cracks remained sharp [11]. Pashley et al. [15] have reported elastic moduli of ~253 MPa for dentin dried in air, substantially higher

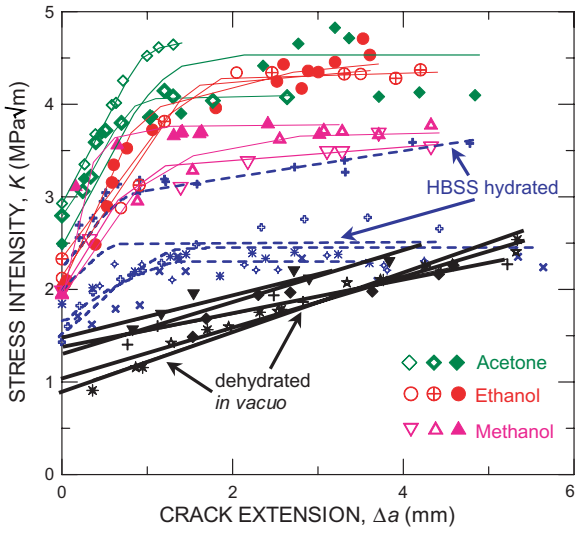

Fig. 9. Fracture resistance of dentin for chemically dehydrated dentin tested in acetone, ethanol and methanol and for HBSS-hydrated dentin (dotted lines) are shown together with similar data for dentin dehydrated in vacuo. Data for hydrated and in vacuo dehydrated dentin is from a previous study [11].

than that measured in water (11 MPa) and even in acetone (132 MPa), which would be consistent with a greater ease of collagen–collagen hydrogen bonding with very little fluid intervening. However, the total elimination of fluid also appears to prevent the plastic and viscoplastic (creep) crack blunting deformation observed in Ref. [11], which would lead to much higher local stresses near the crack tip for the in vacuo case. Thus, any improved intermolecular bonding is offset by the fact that the greatly reduced deformability leads to higher local crack-tip stresses, and accordingly dentin becomes embrittled in the absence of any fluid. Indeed, in chemically dehydrated dentin, crack blunting deformation was observed (both directly using optical microscopy and also inferred from the bilinear R-curve behavior), making the fracture behavior more similar to the hydrated case than the in vacuo case, as evidenced by the *qualitatively* similar appearance of the chemically dehydrated R-curves as compared to hydrated dentin (Fig. 1). However, further research is necessary to better understand the viscoplastic deformation behavior in the presence of fluid in dentin.

5. Conclusions

Based on a study of the in vitro fracture and deformation behavior of elephant dentin which has been chemically dehydrated using various common polar solvents (acetone, methanol, ethanol), the following conclusions can be made:

1. Chemical dehydration with common anhydrous solvents with decreasing hydrogen bonding ability (as measured by the Hansen solubility parameter for hydrogen bonding, δ_H) causes increases the fracture resistance behavior of dentin, involving enhancement to both the intrinsic (crack-initiation) and extrinsic (crack-growth) toughness. This behavior is found to be reversible, and is thought to be related to increased intermolecular hydrogen bonding upon the replacement of water with weaker hydrogen bond forming solvents.
2. The increase in the intrinsic toughness was attributed to increased hydrogen bonding causing the collagen molecules and fibrils to be more tightly bound near the crack tip, thereby preventing premature failure and crack extension. This is consistent with the enhanced three-point bending failure strengths observed for the dentin dehydrated by polar solvents.
3. Increases in the extrinsic (crack-growth) toughness were rationalized in terms of the increased strength and stiffness of the uncracked bridges in the crack wake, which again was thought to be caused by the additional hydrogen bonding in the presence of the polar solvents. Such strength and stiffness increases were reversible and were confirmed through three-point bending and nanoindentation experiments.
4. Although in its natural state, dentin is hydrated with an aqueous fluid, the present results give insight into how water hydration controls the fracture properties. Indeed, while presence of a fluid appears to be vital to allow deformability of dentin, the high hydrogen bonding ability of water appears to excessively "plasticize" the collagen, as compared to other polar solvents with lower hydrogen bonding capabilities, resulting in lower strength, stiffness, and fracture resistance.

Acknowledgement

This work was supported by the National Institutes of Health under Grant No. P01DE09859 (for RKN and MB), by the Director, Office of Science, Office of Basic Energy Science, Division of Materials Sciences and Engineering, US Department of Energy under No. DE-AC03-76SF00098 (for JWA, JJK and ROR), and by the Laboratory Science and Technology Office, LLNL, under the auspices of the US Department of Energy W-7405-ENG48 (for JHK). The authors also wish to thank Profs. S.J. and G.W. Marshall for their support, Dr. A.P. Tomsia for helpful discussions, Ms. C. Kinzley, Curator, Oakland Zoo, Oakland, CA for supplying the dentin, Dr. Y. Borodko for use of the UV Raman system, and Ms. G. Nonomura for help with sample preparation for the AFM work. JJK would also like to thank Mr. W. Ewing for useful discussions.

References

[1] Hodge AJ, Petruska JA. Recent studies with the electron microscope on ordered aggregates of the tropocollagen molecule. In: Ramachandran GN, editor. Aspects of protein structure. Academic Press; 1963. p. 289.
[2] Ten Cate AR. Oral histology—development, structure and function. Mosby; 1994, p. 173.
[3] van der Graaf E, Ten Bosch J. Arch Oral Biol 1990;35:731.
[4] Chapman GE, McLauchlan KA. Proc R Soc London B 1969;173:223.
[5] Lazarev YA, Grishkovsky BA, Khromova TB, Lazareva AV, Grechishko VS. Biopolymers 1992;32:189.
[6] Chapman GE, Danyluk SS, McLauchlan KA. Proc R Soc London B 1971;178:456.
[7] Ramachandran GX, Chandrasekharan R. Biopolymers 1968;6:1649.
[8] Lazarev YA, Grishkovsky BA, Khromova TB. Biopolymers 1985;24:1449.
[9] Bella J, Eaton M, Brodsky B, Berman HM. Science 1994;266:75.
[10] Bella J, Brodsky B, Berman HM. Structure 1995;3:893.
[11] Kruzic JJ, Nalla RK, Kinney JH, Ritchie RO. Biomaterials 2003;24:5209.
[12] Nakabayashi N, Pashley DH. Hybridization of dental hard tissues. Quintessence Publishing Co. Ltd.; 1998.
[13] Maciel KT, Carvalho RM, Ringle RD, Preston CD, Russell CM, Pashley DH. J Dent Res 1996;75:1851.
[14] Pashley DH, Agee KA, Nakajma M, Tay FR, Carvalho RM, Terada RSS, et al. J Biomed Mater Res 2001;56:273.
[15] Pashley DH, Agee KA, Carvalho RM, Lee K-W, Tay FR, Callison TE. Dent Mater 2003;19:347.
[16] Hansen CM. Hansen solubility parameters: a user's handbook. CRC Press; 2000.
[17] Kahler B, Swain MV, Moule A. J Biomech 2003;36:229.
[18] Nalla RK, Kruzic JJ, Ritchie RO. Bone 2004;34:790.
[19] Raubenheimer EJ, Dauth J, Dreyer MJ, Smith PD, Turner ML. S Afr J Sci 1990;86:192.
[20] ASTM E399-90 (Reapproved 1997). Annual book of ASTM Standards, vol. 03.01: Metals—mechanical testing; elevated and low-temperature tests; metallography. West Conshohocken, PA, USA: ASTM; 2002.
[21] Saxena A, Hudak Jr SJ. Int J Fract 1978;14:453.
[22] Balooch M, Demos SG, Kinney JH, Marshall GW, Balooch G, Marshall SJ. J Mater Sci—Mater Med 2001;12:507.
[23] Strojny A, Xia X, Tsou A, Gerberich WW. J Adhes Sci Technol 1998;12:1299.
[24] Sneddon IN. Int J Eng Sci 1965;3:47.
[25] Pharr GM, Oliver WC, Brotzen FR. J Mater Res 1992;7:613.
[26] Marshall GW, Marshall SJ, Balooch M, Kinney JH. Methods Mol Biol 2004;242:141.
[27] Bandekar J. Biochim Biophys Acta 1992;1120:123.
[28] Lucksanambool P, Higgs WAJ, Higgs RJED, Swain MW. Biomaterials 2001;22:3127.
[29] Carden A, Morris MD. J Biomed Opt 2000;5:259.
[30] Carden A, Rajachar RM, Morris MD, Kohn DH. Calcif Tissue Int 2003;72:166.
[31] Asmussen E, Hansen EK, Peutzfeldt A. J Dent Res 1991;70:1290.
[32] Asmussen E, Uno S. J Dent Res 1993;72:558.
[33] Finger WJ, Inoue M, Asmussen E. Am J Dent 1994;7:35.
[34] Miller RG, Bowles CQ, Chappelow CC, Eick JD. J Biomed Mater Res 1998;41:237.
[35] Chappelow CC, Power MD, Bowles CQ, Miller RG, Pinzino CS, Eick JD. Dent Mater 2000;16:396.
[36] Chawla KK. Composite materials science and engineering. New York: Springer-Verlag, Inc.; 1987, p. 292.
[37] Gupta A, Mehrotra R, Tewari J, Jain RM, Chauhan VS. Biopolymers 1999;50:595.
[38] Nalla RK, Kinney JH, Ritchie RO. Biomaterials 2003;24:3955.